ECMOR XIV

Th A44

Robust Ensemble-based Multi-objective Optimization

R.M. Fonseca* (Delft University of Technology), A.S. Stordal (IRIS), O. Leeuwenburgh (TNO), P.M.J. Van Den Hof (Eindhoven University of Technology) & J.D. Jansen (Delft University of Technology)

SUMMARY

We consider robust ensemble-based multi-objective optimization using a hierarchical switching algorithm for combined long-term and short term water flooding optimization. We apply a modified formulation of the ensemble gradient which results in improved performance compared to earlier formulations. We also apply multi-dimensional scaling to visualize projections of the high-dimensional search space, to aid in understanding the complex nature of the objective function surface and the performance of the optimization algorithm. This provides insights into the quality of the gradient, and confirms the presence of ridges in the objective function surface which can be exploited for multi-objective optimization. We used a 18553-gridblock reservoir model of a channelized reservoir with 4 producers and 8 injectors. The controls were the flow rates in the injectors, and the long-term and short-term objective functions were undiscounted net present value (NPV) and highly discounted (25%) NPV respectively. We achieved an increase of 15.2% in the secondary objective for a decrease of 0.5% in the primary objective, averaged over 100 geological realizations. The total number of reservoir simulations was around 20000, which indicates the potential to use the ensemble optimization method for robust multi-objective optimization of medium-sized reservoir models.

Introduction

Various model-based optimization studies have shown the potential of using optimal control theory for dynamic optimization of petroleum systems, thereby improving overall reservoir management. Most of these studies used a single reservoir model to optimize a single life-cycle (i.e. long-term) objective. The resulting operating strategies are suboptimal, however, since in reality well and field operation strategies are typically based on operational production criteria such as delivery contracts, which are governed by much shorter time horizons (days to weeks or months) than life-cycle objectives (years to decades). In fact, strategies that optimize short-term operational objectives are often in conflict with optimal long-term strategies. A second reason for sub-optimality is the inherent uncertainty present in the geological and petro-physical modeling that forms the basis for the reservoir model. This uncertainty will translate into a distribution of possible objective values which cannot be adequately characterized by a single model outcome.

Several authors observed that near-identical life-cycle objective function values could be obtained by significantly different strategies. This led to the inference that the life-cycle optimization problem is ill-posed and has non-unique solutions. Another way to look at this is that the problem contains redundant degrees of freedom (DOFs) in the inputs that can be exploited to optimize one or multiple additional objectives. This idea, together with the (indirect) indication that the DOFs appear to manifest themselves as ridges in the objective function, formed the basis for the hierarchical multi-objective optimization structure proposed by Van Essen et al. (2011). They introduced two approaches to solve the hierarchical optimization structure. The first one is a theoretical null-space approach which is computationally very demanding since it requires building a Hessian matrix of the primary objective function. The second approach is a practical alternative which uses a switching function. Both approaches resulted in a significant increase in a short-term (secondary) objective with minimal change to the life-cycle (primary) objective function when using a single geological realization.

As argued above incorporating geological uncertainty into the optimization is essential to achieve results of significant realistic and practical value. Many different engineering applications have dealt with uncertainty in modeling and control. Van Essen et al. (2009) described various existing techniques and introduced a ‘robust’ life-cycle optimization workflow in which uncertainty is represented by a large number of equally probable model realizations.

Van Essen et al. (2009; 2011) used the adjoint formulation for gradient-based optimization, following earlier work by Brouwer and Jansen (2004), Sarma et al. (2005) and others; see Jansen (2011) for an overview. The adjoint approach is computationally very efficient, since it requires only one adjoint simulation to compute the gradient, but has the disadvantage that its implementation requires access to the simulation code which is not possible for commercial simulators. Chen et al. (2009) introduced an ensemble-based life-cycle optimization method (EnOpt), which, albeit computationally less attractive, has proven to be a good practical alternative to the adjoint because it is relatively easy to implement and is independent of the reservoir simulator. Do and Reynolds (2013) recently provided an analysis of the EnOpt method and demonstrated its close connection to other stochastic gradient estimation techniques such as simultaneous perturbation stochastic approximation (SPSA) and the simplex gradient method.

The concept of robust optimization within the EnOpt framework was discussed in Chen (2008) and Chen and Oliver (2010) where they used two ensemble sets: an ensemble of controls and an ensemble of geological models. Intuitively, if the two ensembles consist of M members each, we would require M^2 function evaluations for a gradient estimate which is computationally not attractive. Chen (2008) provides an argumentation for the possibility of evaluating only M samples in order to approximate the robust EnOpt gradient which would make EnOpt computationally very attractive for robust optimization. Thus if, hypothetically, geological uncertainty were captured in an ensemble of M

realizations, we would need only *M* perturbed control samples, where each geological realization is coupled to one control sample, i.e. in a 1:1 ratio, to estimate a "robust gradient". Hereafter this will be referred to as the "original formulation". In Stordal et al. (2014) it is shown how this implementation converges to the exact gradient in a natural evolutionary framework.

Fonseca et al. (2014) investigated the applicability of EnOpt for multi-objective optimization based on a single model realization and showed results which suggest that EnOpt is a viable alternative when the adjoint is unavailable. Furthermore, the robust EnOpt implementation as introduced by Chen et al. (2008), which uses a 1:1 ensemble ratio, is computationally competitive to the adjoint method, because one adjoint simulation is required for each model realization. Chen et al. (2009) reported a successful application of this approach to the SPE Brugge benchmark case.

Recently, Chen et al. (2012) presented a robust multi-objective optimization scheme and Capolei et al. (2013) suggested a modification for a life-cycle robust optimization scheme both using adjoint gradients. Additionally, Raniolo et al. (2013) and Li et al. (2012), have investigated the applicability of approximate gradient techniques for life-cycle robust water flooding optimization while Yang et al. (2011) applied the robust optimization principle to a Steam-Assisted Gravity Drainage (SAGD) application. Yasari et al. 2013, Pajonk et al. 2011, Schulze-Riegert et al. (2011) and Awotunde and Sibaweihi (2011) have investigated the applicability of robust multi-objective optimization using evolutionary algorithms for well control and well placement optimization with objectives varying from economic criteria to voidage replacement ratio and cumulative production volumes.

In this paper we investigate the applicability of an ensemble-based robust hierarchical multi-objective optimization framework. As mentioned above, the success of multi-objective optimization has been attributed by some to the presence of ridges in the objective function. While this idea is confirmed indirectly by the results of Van Essen et al. (2011), direct visualization the objective function space is challenging, if not practically impossible, for high-dimensional problems. Insights into the nature and shape of the objective function space can be particularly useful for verifying the success of the optimization process and the quality of the gradient estimates, especially when working with approximate gradients. We therefore also investigate the possibility of visualizing an approximation (projection) of the objective function through a multi-dimensional scaling (MDS) approach.

Different gradient formulations

Recently there has been an increase in the application and understanding of the ensemble-based robust gradient estimate. The original formulation with the 1:1 ensemble ratio described above has not always lead to results of satisfactory value. Different studies have suggested variations to the original formulation to improve the robust gradient estimate. In the following section we provide, to the best of our knowledge, a complete overview of the existing different variations. A comparison of the performance of these variations is described in the numerical results below.

Selected models approach

Raniolo et al. (2013) did not achieve optimized results of any significant value when using the original formulation which they reasoned to be the result of a poor gradient estimate. To counter this they proposed the use of a set of five selected models which would approximately capture the geological uncertainty. This method of selecting a subset of models based on a ranking criteria was also used by Yang et al. (2011). This subset of five models was chosen to roughly represent two P10 models, two P90 models and one P50 model. Raniolo et al. (2013) used the EM algorithm to rank the geological realizations while Yang et al. (2011) used direct numerical simulation of a SAGD process for the ranking. With this set of models, they then coupled each model with multiple control samples to estimate different individual gradients (akin to deterministic optimization), the summation of which results in a single robust gradient. With this approach they achieved better results than with the original formulation. They suggest that using the 1:1 ratio is not sufficient for a good gradient estimate and that by changing the ratio better gradient estimates can be obtained. In this paper we use

a ratio of 1:20, i.e. each realization is coupled with 20 control samples. Note that the set of selected models remain fixed throughout the optimization and that a different subset of model realizations could lead to different results. In this study we used a reactive control based performance to rank and choose the set of models.

Random models approach

Li et al. (2012), using the SPSA technique to approximate a gradient, suggested to randomly select a subset of models at every iteration of the optimization, instead of using an a-priori chosen subset of models. With this randomly chosen set, similar to the selected models approach, individual gradients are estimated to estimate a single robust gradient. With this random selection of models there is no definitive way to enforce that the selected models in any way capture the uncertainty or that all model realizations are chosen at least once during the optimization. In our study we have used the concept of randomly selecting a subset of models at every iteration with the gradient being estimated by the EnOpt method. We have used five randomly selected models at each iteration and coupled each model with 20 control samples, i.e. a ratio of 1:20 to estimate the gradient.

Reactive optimization

Dehdari and Oliver 2012 showed that, for a deterministic optimization case using EnOpt, better results can sometimes be obtained when reactive control is included within the optimization. Reactive control is the simulator-controlled shut-in of producers once their production reaches an uneconomic water cut. More recently, Capolei et al. (2013) also reported better solutions for adjoint-based robust optimization when reactive control is included within the optimization. However, in their original formulation (i.e. without including reactive control) they used bound constraints on the controls for the producers that were so tight that the producers could never be shut-in.

Modified formulation

Do and Reynolds (2013) proposed a modified EnOpt for deterministic optimization wherein the control and objective function anomalies are computed with respect to the distribution mean i.e. the current control vector and the corresponding objective function values rather than the sample mean as is done in the original formulation. We further propose a small modification to this formulation, wherein the objective function anomalies are now computed with respect to the objective function value of the current control for an individual model realization. This modification leads to a different weighting scheme for the gradient estimate wherein each realization has a weighting depending on the relative increase or decrease of their objective function values compared to the objective function values of the perturbed control applied to the same realization. Thus the effect of realizations (outliers) whose objective function values dominate the expected value is reduced. The 1:1 ratio still holds for this gradient formulation.

Visualization of the objective function space

When dealing with high-dimensional optimization problems, knowledge of the objective function space is very limited and visualization of the space is impossible. Information about the nature and shape of the objective function space can be very useful in interpreting and understanding optimization results. MDS described in Borg and Groenen (1997) is a technique used in various sciences to cluster and represent projections of multi-dimensional data sets in two dimensions based on a distance metric between the data sets. Thus using MDS it is possible to project a set of high-dimensional well controls onto a $\mathbb{R}^2$ space and then plot the objective function as a function of two variables with approximately the same distance between the points and the original controls. This leads to a three-dimensional (3D) plot with MDS distances on the x and y axes and the objective function values of each point on the z axis. This gives us an approximation of the objective function which can provide useful insights and knowledge about the presence of local optima, ridges and

valleys, gradient quality etc. in the optimization search space. The MDS algorithm can be described by the following.

For a given set of variables, $\{x_i\}_{i=1}^N$, in a high dimensional space χ with dim(χ) >> N we can construct a distance matrix **S** where $s_{ij} = \|x_i - x_j\|_\chi$. Then the MDS algorithm finds points, $\{y_i\}_{i=1}^N$, in $\mathbb{R}^d$, with $d \leq N$, that minimize $|s_{ij} - k_{ij}|, i, j = 1, \ldots, N$ where k_{ij} is the Euclidean distance between y_i and y_j. If **S** is positive definite, the points $\{y_i\}_{i=1}^N$ can be found from a singular value decomposition of a squared twice-centred version of **S**. For the production optimization examples considered in this paper, we sample points (controls) from a Gaussian density with mean from the final iteration of the optimization and a covariance that is larger than the covariance used in the final iteration of the optimization algorithm. The objective function is then calculated for each of these controls and plotted against the MDS points in $\mathbb{R}^2$. This help us to approximate the shape and nature of the objective function in a neighbourhood (locally) around our optimized solution.

Numerical example

A 3D synthetic reservoir model was used to test the robust ensemble based multi-objective optimization methods. The life cycle of the reservoir covers a time span of 3600 days or 10 years. The objective function J, representing Net Present Value (NPV), is defined in the usual way as

$$J = \sum_{k=1}^{K} \left(\frac{\left\{ \left[(q_{o,k}) \cdot r_o - (q_{wp,k}) \cdot r_{wp} \right] - \left[(q_{wi,k}) \cdot r_{wi} \right] \right\} \cdot \Delta t_k}{(1+b)^{t_k / \tau_t}} \right), \qquad (1)$$

where $q_{o,k}$ is the oil production rate in bbl/day, $q_{wp,k}$ is the water production rate in bbl/day, $q_{wi,k}$ is the water injection rate in bbl/day, r_o is the price of oil produced in \$/bbl, r_{wp} is the price of water produced in \$/bbl, r_{wi} is the price of water injected in \$/bbl, Δt_k is the difference between consecutive time steps in days, b is the discount factor expressed as a fraction per year, t_k is the cumulative time in days corresponding to time step k, and τ_t is the reference time for discounting (365 days). Following Van Essen et al. (2009), we have chosen two different objective functions, one which highlights the long-term or life-cycle performance of the field and the other to describe the short-term goals for the project. The long-term performance is represented by an undiscounted (0%) NPV, while the short-term goals are accounted for using a highly discounted (25%) NPV.

The model, illustrated in Figure 1, was introduced in Van Essen et al. (2009) along with an ensemble of equi-probable geological scenarios, six of which are illustrated in Figure 2. The models represent a channelized depositional system in the form of discrete permeability fields modeled with $60 \times 60 \times 7 = 25.200$ grid cells of which 18.553 cells are active. A detailed description of a standardized version of this "egg model" is given in Jansen et al. (2013). The uncertainty in the models is described by the different channel orientations and permeability fields of the models. The model is produced using eight peripheral water injection wells and four production wells which are completed in all seven layers. The reservoir and fluid properties used for all ensemble members are given in Table 1. No capillary pressures are included and the reservoir rock is assumed to be incompressible.

We use a commercial fully implicit black oil simulator (Eclipse, 2011) for the reservoir simulations in combination with (robust) EnOpt algorithms to compute the gradient of J with respect to the controls **u**. The gradient is used in a simple steepest ascent scheme, where we determine the step size with the aid of an inexact line search and the Arjimo conditions (Nocedal and Wright 2006). We use the switching approach for hierarchical multi-objective optimization with implementation details as described in Fonseca et al. (2014).

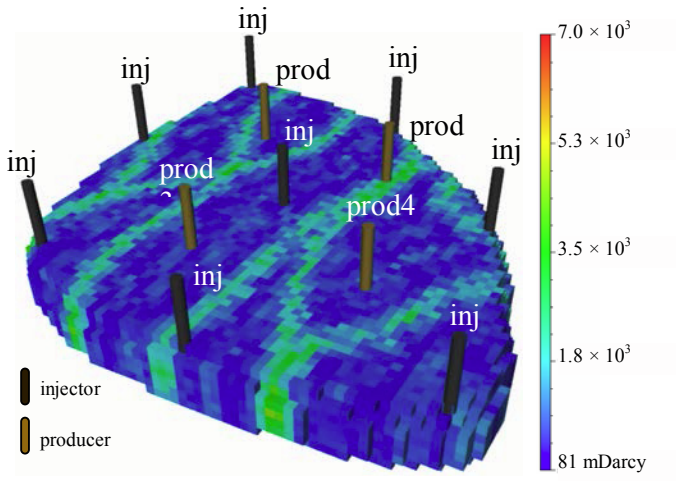

Figure 1 *Permeability field of one ensemble member used for robust optimization.*

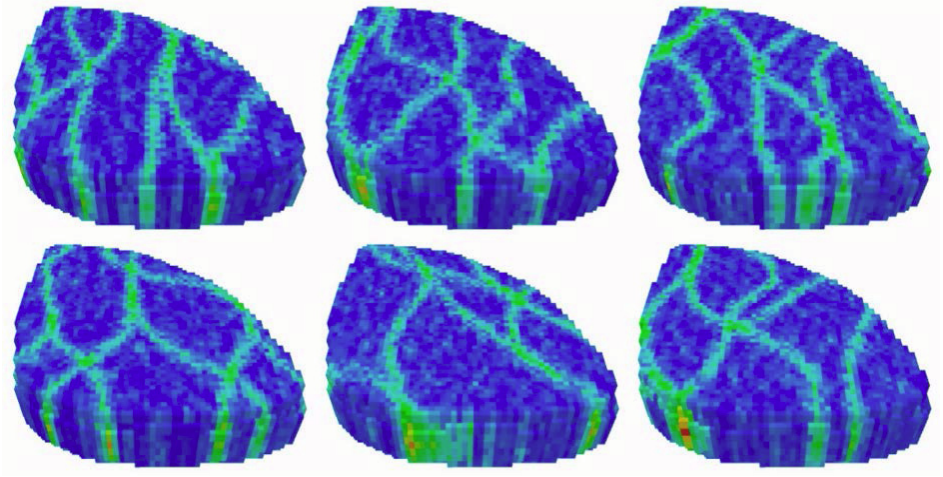

Figure 2 *Illustration of 6 randomly chosen different geological members from an ensemble of 100 equi-probable models (first introduced in Van Essen et al 2009).*

Life-cycle optimization

Water injection rates are the controls to be optimized with a maximum allowable injection rate per well fixed at 60 m^3/day and a minimum rate of 0 m^3/day. The producers are operated at a minimum bottom hole pressure of 385 bars without rate constraints. The producing life of the reservoir is divided into 40 optimization time intervals of 90 days each, and the control vector **u** has therefore $N = 8 \times 40 = 320$ elements. An optimal life-cycle strategy of injection rates for the individual wells is obtained by optimizing the NPV as described in equation (1), with $r_o = 126$ \$/m^3, $r_{wp} = 19$ \$/m^3, and $r_{wi} = 5$ \$/m^3. The discount rate b is set to 0. The initial strategy (starting point) of the life-cycle optimization is a control vector with maximum injection flow rates at all control times. Figure 3 illustrates the optimization process where the blue lines represent the evolution of the objective function values for the 100 different geological realizations during the iterations while the red line is the expected value of the ensemble. The optimized expected objective function value is approximately 42.4 million \$. Due to a lack of significant change in the objective function value the optimization process was terminated after approximately 70 iterations.

Table 1 *Reservoir and fluid properties (from Jansen et al. 2013)*

Symbol	*Variable*	*Value*	*SI units*
h	Grid-block height	4	m
Δx, Δy	Grid-block length/width	8	m
ϕ	Porosity	0.2	-
c_o	Oil compressibility	1.0×10^{-10}	Pa^{-1}
c_w	Water compressibility	1.0×10^{-10}	Pa^{-1}
μ_o	Oil dynamic viscosity	5.0×10^{-3}	Pa s
μ_w	Water dynamic viscosity	1.0×10^{-3}	Pa s
ρ_o	Oil Density	900	kg/m^3
ρ_ω	Water Density	1000	kg/m^3
k_{ro}^0	End-point relative permeability, oil	0.8	–
k_{rw}^0	End-point relative permeability, water	0.75	–
n_o	Corey exponent, oil	4.0	–
n_w	Corey exponent, water	3.0	–
S_{or}	Residual-oil saturation	0.1	–
S_{wc}	Connate-water saturation	0.2	–
$\breve{p}_R$	Initial reservoir pressure (top layer)	40×10^6	Pa
$S_{w,0}$	Initial water saturation	0.1	–
r_{well}	Well-bore radius	0.1	m
T	Simulation time	3600	d

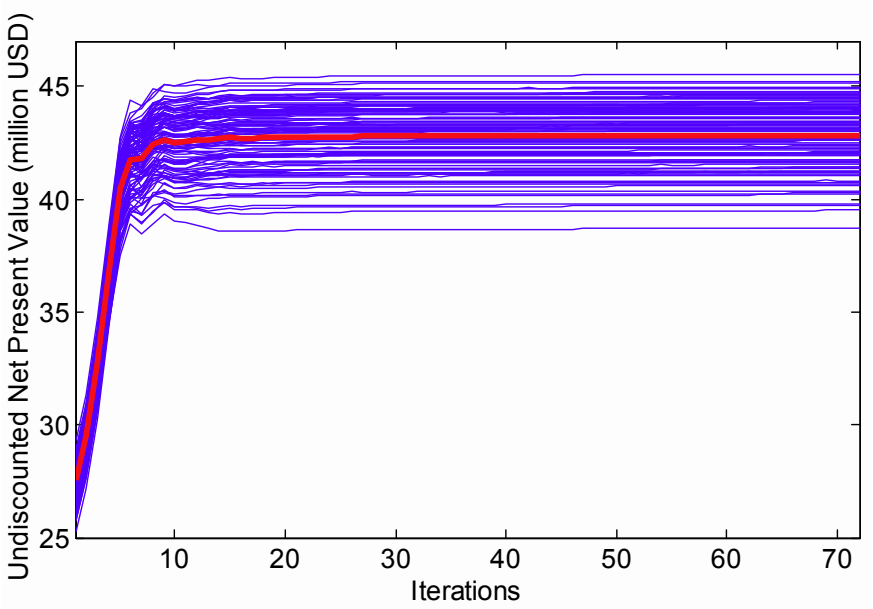

Figure 3 *Objective function values during the optimization procedure for the original robust EnOpt formulation. Red: average value of the ensemble. Blue: individual ensemble members.*

Objective function space

To visually inspect the optimized solution we would need to plot its position in the objective function space, but visualization of such a high-dimensional space is impossible. Therefore, we apply MDS, as described in the theory section, to plot projections of the objective function space as illustrated in Figure 4. The blue dots are control samples created around the optimized solution (red dot) achieved by EnOpt. As can be seen from Figure 4, the optimized solution achieved by EnOpt (red dot) is probably stuck at a local optimum. Interestingly there are many other points (blue dots) which have achieved higher objective function values thus indicating the scope for further optimization. The difference between the highest and lowest expected objective function values of the blue dots is 3.4%, thus indicating the space is not flat. The plot also indicates the presence of ridges which could be utilized for multi-objective optimization. Note: to generate this plot we required 10,000 reservoir simulations.

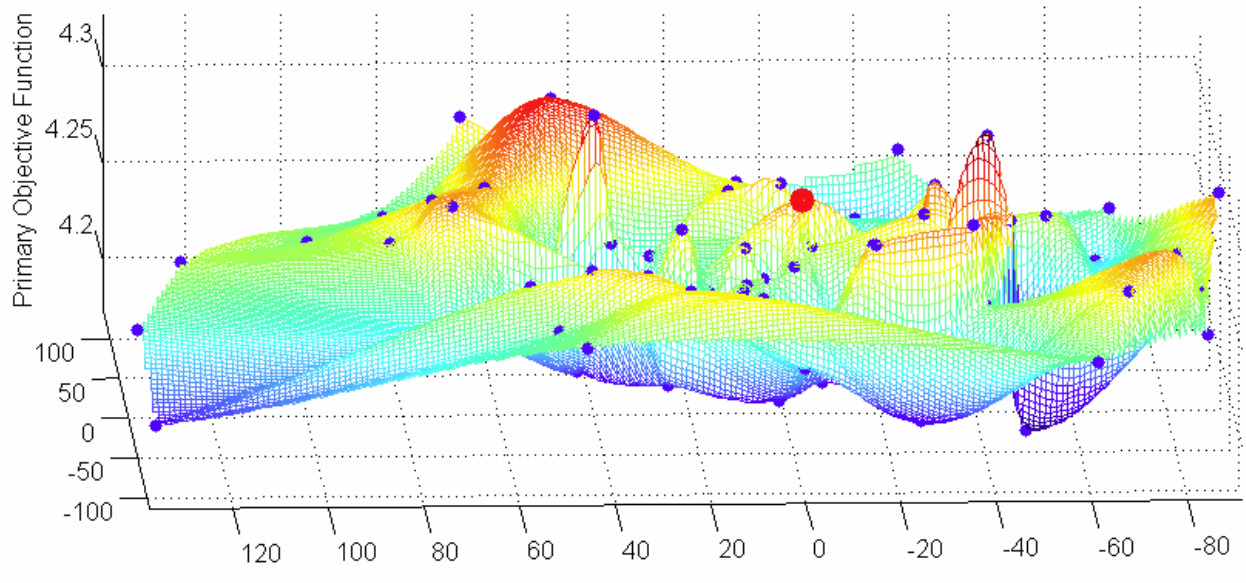

Figure 4 *MDS plot of the mean objective function search space of the primary objective (undiscounted NPV). The red dot is the expected value of the optimized solution achieved in Figure 3.*

Comparison of different gradient formulations

To find solutions that achieve higher objective function values than the one in Figure 4 we investigate the application of various robust gradient formulations discussed in the theory section. In addition, we apply a reactive control strategy, in which the producers are a shut-in when they reach an unprofitable water cut (87 % for the economic values in our example). Figure 5 depicts the objective function values obtained by applying the different formulations. We observe that the original formulation (1:1 ratio) achieves a solution inferior to the traditional reactive control approach. However, it should be noted that the optimization only influences injection rates, whereas the reactive control operates at the producers. The "random models approach" achieves the worst solutions for this example. The "selected model approach" leads to a solution which achieves an expected value 2.5% higher than the original formulation. The "reactive optimization approach" i.e. the ad-hoc procedure to incorporate reactive control in the optimization gives better solutions than reactive control alone. This is to be expected because now the starting point of the optimization is the reactive control solution itself, thus for a worst case scenario we would, with this method, always be at least equal to the reactive control solution. The modified robust formulation achieves the highest expected objective function value which is approximately 3.5% higher than the value for reactive control and 4.5% higher than the value for the original formulation. The modified gradient formulation, like the original formulation, uses the entire ensemble of geological realizations, i.e. it accounts for all the uncertainty available to estimate the robust gradient, unlike the selected models or random models approach.

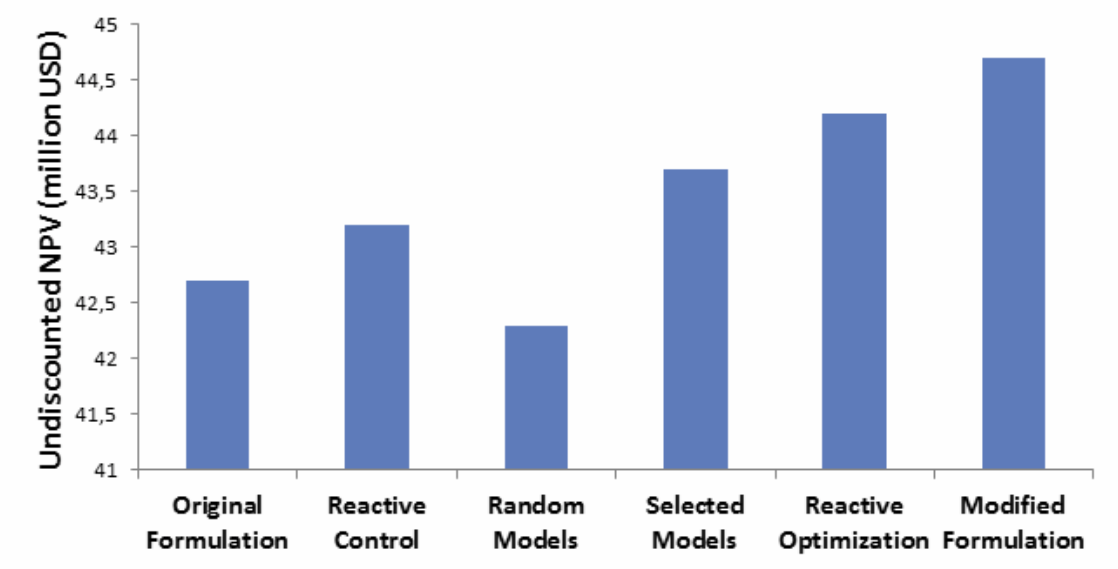

Figure 5 *Comparison of the optimized objective function values for different ensemble-based robust gradient formulations*

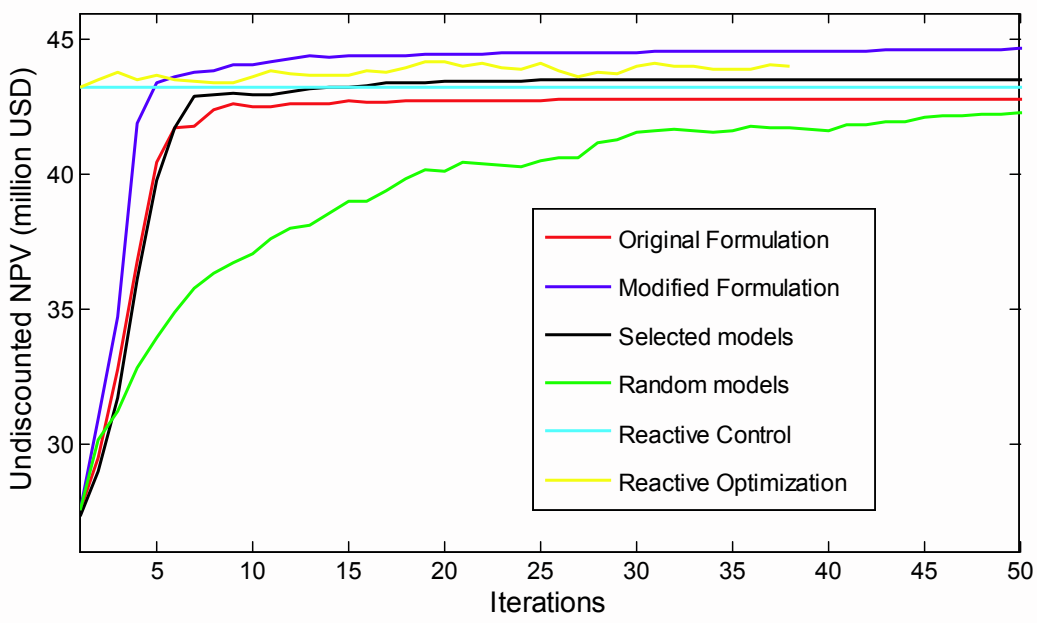

Figure 6 *Objective function values during the optimization procedure for various EnOpt formulations and for reactive control.*

Objective function space for modified robust gradient formulation

Figure 7 is an illustration of the nature of the objective function search space around the optimized solution (red dot) achieved by the modified robust formulation which obtained the best solution compared to other methods for this example. The biggest difference between Figures 4 and 7 is that in Figure 7 there is no solution with a higher value than the optimized solution (red dot). However, it also appears as if the presence of ridges is less than in Figure 4, although the optimized solution still appears to be connected to ridge stretching towards the left. Note that the difference between the minimum and maximum objective function values in Figure 7 is only 1%, which is much less than in Figure 4. For the generation of this plot we used 1000 points which is 10 times more than for Figure 4. It will require further research to establish a better understanding of the relationship between the smoothness of the projected objective function surface and the number of points used to generate it.

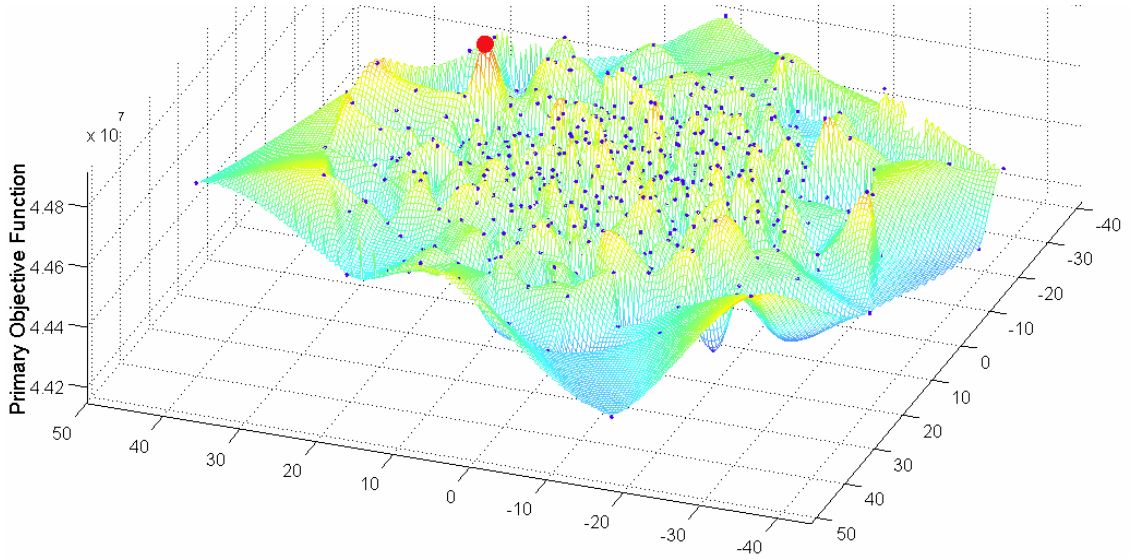

Figure 7 *Plot of the objective function space of the primary objective function around the optimized solution (red dot) achieved with the modified robust gradient formulation.*

Hierarchical switching optimization

The hierarchical switching optimization method is used to achieve multi-objective optimization under uncertainty as illustrated in Figure 8. We observe a mean increase of approximately 15.2% in the secondary objective function (highly discounted NPV) compared to a marginal allowable mean decrease of 0.5% in the primary objective function. The switching optimization begins from the optimized solution achieved by the modified robust gradient formulation for life-cycle optimization. The same modified formulation is also used for this hierarchical optimization. The results illustrates the use of ensemble-based multi-objective optimization under geological uncertainty to achieve results of practical importance. Note: we have terminated the optimization for the secondary objective function after 100 iterations which translates to 10,000 reservoir simulations for the gradient estimate and 10107 simulations for evaluation of the updated control set, i.e. a total of 20,107 reservoir simulations.

Figure 9 depicts a comparison of the mean cumulative cash flow over time for the optimized solutions achieved by the switching algorithm (blue), life-cycle optimization (green) and reactive control (red). It is observed that after 500 days the cumulative cash flow with life cycle optimization is approximately 10.3 million $ compared to the control strategy obtained with switching optimization which achieves a cash flow of 15.7 million $. This 52% increase of 5 million $ over 500 days will enable the project to achieve the break-even point faster. Similar to the results obtained in Fonseca et al. (2014) the reactive control strategy gives the best short-term performance while the switching algorithm, although inferior to reactive control, leads to an improved short-term performance compared to the optimized life-cycle strategy.

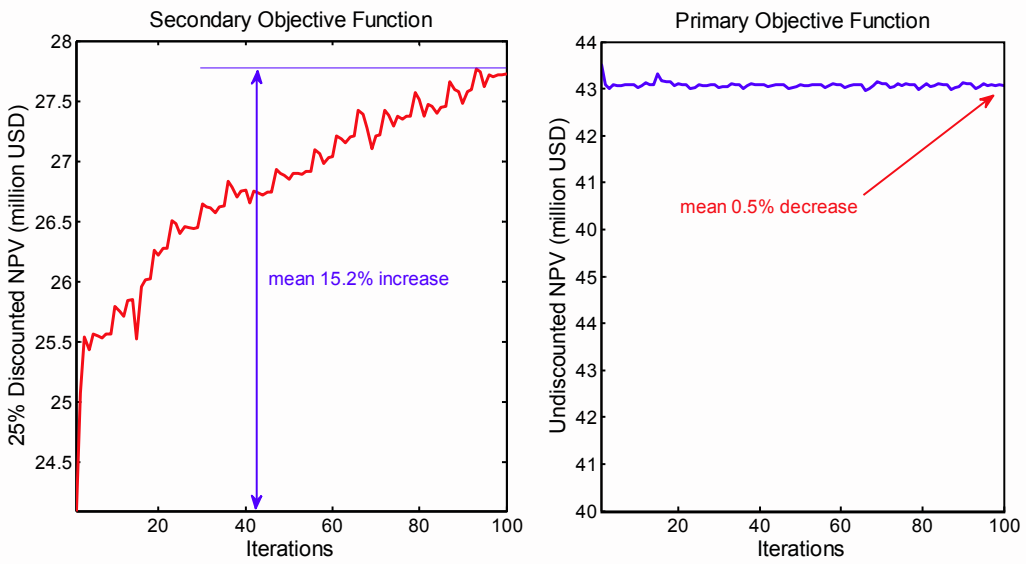

Figure 8 *Illustration of hierarchical switching optimization of the secondary objective function (red) and the corresponding decrease in the primary objective function (blue) starting from the optimized solution achieved with the modified robust formulation.*

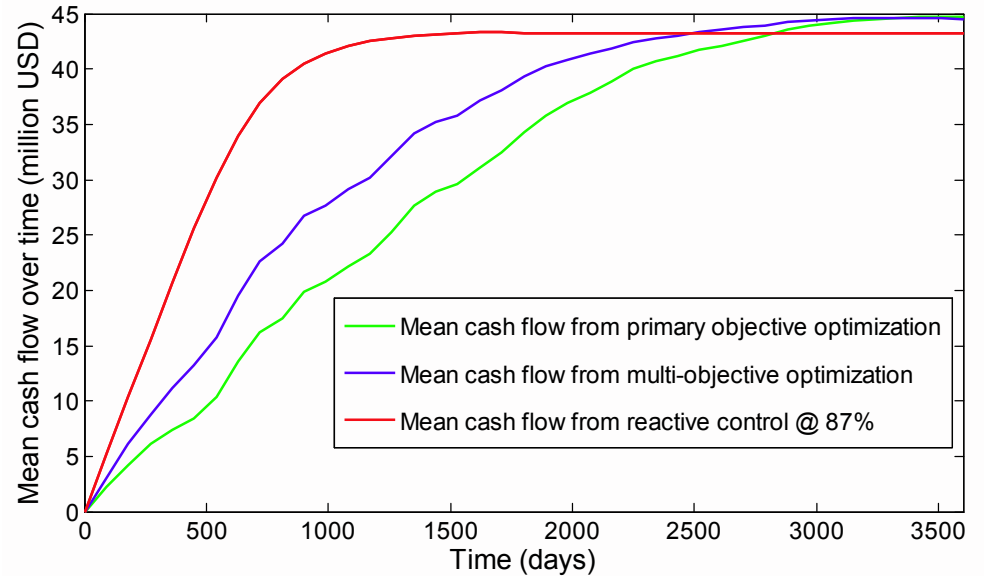

Figure 9 *Comparison of the mean cash flow over time for the entire ensemble of geological realization for the different optimization strategies.*

Plotting the optimization path

In Figure 10 we use MDS to track the path (indicated by arrows) of the multi-objective optimization results shown in Figure 8. We observe that we have reached a solution which is not close to the starting point of the optimization for only a minor decrease in the primary objective and a relatively significant increase in the secondary objective.

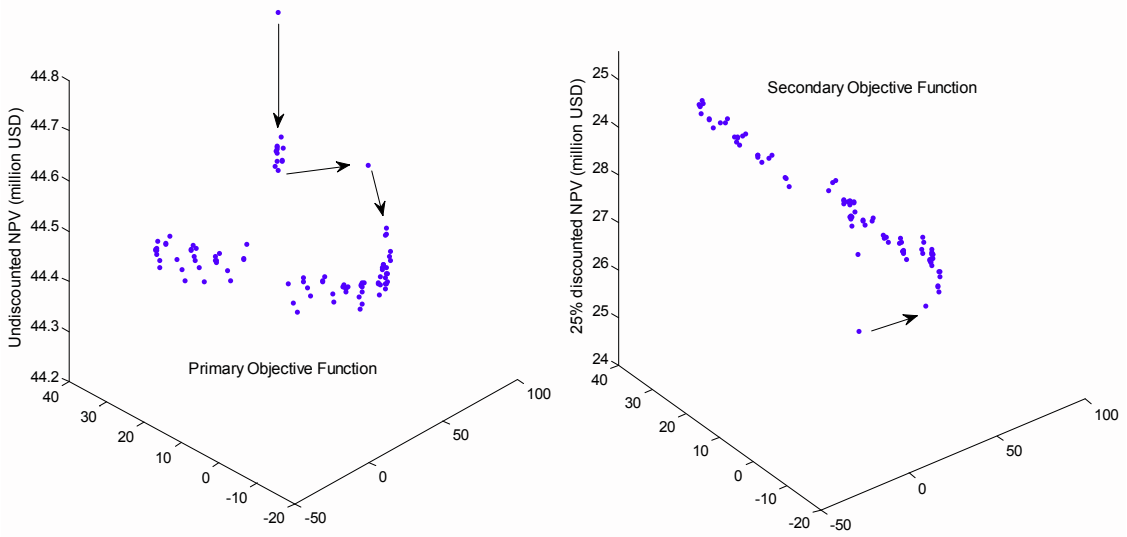

Figure 10 *A comparison of the optimization path for the two objectives, undiscounted NPV (left hand plot) shows a minor decrease in objective function and 25% discounted NPV (right hand plot) shows a significant increase in objective function.*

Conclusions

We investigated the use of various robust EnOpt formulations to perform hierarchical water flooding optimization, for various ratios of the control vector ensemble size to the geological ensemble size. Moreover, we introduced the use of MDS to approximately visualize (projections of) the objective function space. For the example considered in this paper we reach the following conclusions:

- An increase of 15.2% in the expected value of the secondary objective function was achieved with the hierarchical switching algorithm for a 0.5% decrease in the expected value of the primary objective function using a modified ensemble gradient formulation and a 1:1 ensemble ratio.
- The modified formulation based on the 1:1 ensemble ratio is not only computationally attractive but also uses the entire ensemble of geological realizations i.e. captures all the uncertainty available.
- The optimized strategy obtained with the modified formulation achieved a 4.5% increase in the expected objection function value over the strategy obtained by the original formulation and a 3.5% increase over a reactive control strategy.
- The use of MDS provides a useful means to approximately visualize projections of the objective function space. However, it will require further research to establish a better understanding of the relationship between the smoothness of the projected objective function surface and the number of points used to generate it.
- The total number of reservoir simulations was around 20000, which indicates the potential to use the ensemble optimization method for robust multi-objective optimization of medium-sized reservoir models

Acknowledgements

This research was carried out within the context of the ISAPP Knowledge Centre. ISAPP (Integrated Systems Approach to Petroleum Production) is a joint project of TNO, Delft University of Technology, ENI, Statoil and Petrobras. The authors acknowledge Schlumberger for providing multiple academic Eclipse licenses for this work. The second author acknowledges financial support from all industry partners of the National IOR Center of Norway.

References

Awotunde, A.A., and Sibaweihi, N.[2012] Consideration of Voidage Replacement Ratio in Well Placement Optimization. Paper SPE 163354 presented at the SPE Kuwait International Petroleum Conference and Exhibition, Kuwait City, Kuwait, 10-12 December.

Borg, I. and Groenen. P. [1997] Modern multidimensional scaling: theory and applications. Springer. New York.

Brouwer, R. and Jansen, J.D. [2004] Dynamic Optimization of Water Flooding With Smart Wells Using Optimal Control Theory. *SPE Journal* **9**(4) 391-402.

Capolei, A., Suwartadi, E,. Foss, B, and Jørgensen**,** J.B**. [**2013] Waterflooding optimization in uncertain geological scenarios. *Computational Geosciences* **17**(6) 991-1013.

Chen, Y. 2008. Efficient Ensemble based Reservoir Management. PhD Thesis, University of Oklahoma, USA.

Chen, Y. and Oliver, D.S. [2010] Ensemble-Based Closed-Loop Optimization Applied to Brugge Field. *SPE Reservoir Evaluation and Engineering* **13**(1) 56-71.

Chen, C., Li, G. and Reynolds, A. [2012] Robust Constrained Optimization of Short- and Long-Term Net Present Value for Closed-Loop Reservoir Management. *SPE Journal* **17**(3) 849-864.

Chen, Y., Oliver, D.S. and Zhang, D. [2009] Efficient Ensemble-Based Closed-Loop Production Optimization. *SPE Journal* **14**(4) 634-645.

Dehdari, V. and Oliver, D.S. [2012] Sequential Quadratic Programming for Solving Constrained Production Optimization--Case Study From Brugge Field. *SPE Journal* **17**(3) 874-884.

Do, S.T. and Reynolds, A.C. [2013] Theoretical connections between optimization algorithms based on an approximate gradient. *Computational Geosciences* **17** (6) 959-973.

Eclipse [2011] http://www.slb.com/services/software/reseng/eclipse.

Fonseca, R.M., Leeuwenburgh, O. Van den Hof, P.M.J. and Jansen, J.D. [2014] Ensemble-based hierarchical multi-objective production optimization of smart wells. *Computational Geosciences.* Published on-line. DOI: 10.1007/s10596-013-9399-2.

Jansen, J.D. [2011] Adjoint-based optimization of multi-phase flow through porous media – A review. *Computers and Fluids* **46**(1) 40-51.

Jansen, J.D., Fonseca, R.M., Kahrobaei, S.S., Siraj, M.M., van Essen, G.M. and Van den Hof, P.M.J. [2013] The "Egg Model". Research note and data set Delft University of Technology, The Netherlands. http://repository.tudelft.nl/view/ir/uuid:1b85ee17-3e58-4fa4-be79-8328945a4491/ (report); http://data.3tu.nl/repository/uuid:916c86cd-3558-4672-829a-105c62985ab2 (data).

Li, L., Jafarpour, B. and Mohammad-Khaninezhad, M.R. [2012] A simultaneous perturbation stochastic approximation algorithm for coupled well placement and control optimization under geologic uncertainty. *Computational Geosciences* **17**(1) 167-188.

Lorentzen, R.J., Berg, A., Naevdal, G. and Vefring, E.H. [2006] A New Approach for Dynamic Optimization of Waterflooding Problems. Paper SPE-99690-MS presented at the Intelligent Energy Conference and Exhibition, Amsterdam, The Netherlands, 11-13 April 2006.

Nocedal, J. and Wright, S.J. [2006] *Numerical optimzation 2nd ed*. Springer, New York.

Pajonk, O., Schulze-Riegert, R., Krosche, M., Hassan, M. and Nwakile, M.M. [2011] Ensemble-Based Water Flooding Optimization Applied to Mature Fields. Paper SPE-142621-MS presented at the SPE Middle East Oil and Gas Show and Conference, Manama, Bahrain, 25-28 September 2011.

Raniolo, S., Dovera, L., Cominelli, A., Callegaro, C. and F. Masserano [2013] History matching and polymer injection optimization in a mature field using the ensemble Kalman filter. In *Proc. 17th European Symposium Improved Oil Recovery*, St. Petersburg, Russia, 16-18 April.

Sarma, P., Aziz, K. and Durlofsky, L.J. [2005] Implementation of Adjoint Solution for Optimal Control of Smart Wells. Paper SPE 92864 presented at the SPE Reservoir Simulation Symposium, The Woodlands, USA, 31 January–2 February.

Schulze-Riegert, R., Bagheri, M., Krosche, M., Kueck, N. and Ma, D. [2011] Multiple-Objective Optimization Applied to Well Path Design under Geological Uncertainty. Paper SPE-141712-MS presented at the SPE Reservoir Simulation Symposium, The Woodlands, USA, 21-23 February.

Stordal, A.S., Szklarz, S.P. and Leeuwenburgh, O. [2014] A closer look at ensemble based optimization in reservoir management. Proc. 14th European Conference on the Mathematics of Oil Recovery ECMOR XIV, Catania, Italy, 8-11 September.

Van Essen, G., Van den Hof, P. and Jansen, J.D. [2011] Hierarchical long-term and short-term production optimization. *SPE Journal* **16**(1), 191-199.

Van Essen, G., Zandvliet, M., Van den Hof, P., Bosgra, O. and Jansen, J.D. [2009] Robust waterflooding optimization of multiple geological scenarios. *SPE Journal* **14**(1), 202-210.

Yang, C., Card, C., Nghiem, L.X. and Fedutenko, E. [2011] Robust Optimization of SAGD Operations under Geological Uncertainties. Paper SPE-141676-MS presented at the SPE Reservoir Simulation Symposium, The Woodlands, USA, 21-23 February.

Yasari, E., Pishvaie, M.R., Khorasheh, F., Salahshoor, K., Kharrat, R. [2013] Application of multi-criterion robust optimization in water-flooding of oil reservoir. *Journal of Petroleum Science and Engineering* **109** 1–11.